Nuclear Physics A425 (1984) 469–492

THE $^{14}C(\alpha, \alpha')^{14}C$ AND $^{13}C(d, p)^{14}C$ REACTIONS †

R. J. PETERSON, H. C. BHANG*, J. J. HAMILL** and T. G. MASTERSON

Nuclear Physics Laboratory University of Colorado, Boulder, CO 80309, USA

Received 29 December 1983

Abstract: The isoscalar transition rates and neutron-stripping probabilities to states of ^{14}C have been measured using the 35 MeV $^{14}C(\alpha, \alpha')^{14}C$ and 17.7 MeV $^{13}C(d, p)^{14}C$ reactions. States showing great charge asymmetries in pion scattering at 8.32 MeV (2^+) and 11.7 MeV (4^-) were examined in detail. Isoscalar transition rates $B(02)$ were determined to be 168, 96 and 74 fm^4 for the 7.01, 8.32 and 10.45 MeV 2^+ states, with identical single-neutron spectroscopic factors of 0.065, from the (d, p) data, for the lowest two states.

E NUCLEAR REACTIONS $^{14}C(\alpha, \alpha')$, $E = 35$ MeV; $^{13}C(d, p)$, $E = 17.7$ MeV; measured $\sigma(E, \theta)$. Deduced isoscalar transition rates and neutron spectroscopic factors, DWBA analysis.

1. Introduction

The structure of ^{14}C can be simply thought of as due to the two proton holes in ^{16}O or two neutrons beyond ^{12}C. These two extreme isospin compositions may mix, giving, in addition to the usual isoscalar states, levels with the phases of the neutron and proton components such that sensitive cancellations may occur in π^+ or π^- inelastic scattering. Although striking pion scattering results have been published [1]), only for the first few states are the isoscalar transition rates known even approximately [2]). We report here inelastic α-particle scattering yields for many states of ^{14}C.

Another view of the structure of ^{14}C is provided by coupling a single neutron to the ground state of ^{13}C. Earlier neutron stripping results [3]) †† did not examine those states now known from the pion scattering results to be of great interest. We have therefore used the $^{13}C(d, p)^{14}C$ reaction to populate many of the same levels as seen in the α-scattering. Warburton and Pinkston [5]) suggested long ago a

† Supported in part by the US DOE.
* Present address: Physics Department, Seoul National University, Seoul, Republic of Korea.
** Present address: KVI, Groningen, The Netherlands.
†† Earlier $^{13}C(p, d)$ results analysed in the PWBA are summarized in ref. [4]).

comparison of (d, n) and (d, p) yields to determine the isospin properties for $A = 14$. Recent proton stripping results on ^{13}C to the $T = 1$ states of ^{14}N provide half of the required information [6]). The new (d, p) data will also be compared to recent neutron resonance work on a ^{13}C target [7, 8]).

Two states expected on theoretical grounds to have spins of 4^- gave striking asymmetries between inelastic π^+ and π^- scattering [1]). Inelastic electron scattering measurements at 180° have recently confirmed these assignments for the 11.72 and 17.33 MeV levels [9]). Such 4^- states are not accessible to either of the reactions reported here by a single interaction, yet the lower one is observed in the spectra. The cross sections for exciting the 11.7 MeV neutron-like state by the (α, α') and (d, p) reactions are analyzed here in a two-step model. The model and its predictions are treated in sect. 5.

2. Experimental and theoretical methods

Both the (α, α') and (d, p) experiments were performed with beams from the University of Colorado AVF cyclotron, with the ^4He energy at 35.53 MeV and the deuteron energy at 17.7 MeV. Silicon detector telescopes were used for particle and energy determinations, with a 5 mm stopping detector. The energy resolutions were 60 keV FWHM for both reactions.

The ^{13}C targets were highly enriched foils of 100 $\mu g/cm^2$ thickness, while the ^{14}C target † was a self-supporting 90% enriched foil of 140 $\mu g/cm^2$ thickness. A cold trap was used to prevent the buildup of ^{12}C on the ^{14}C target. Scattering and stripping reactions on a natural carbon target provided the energy calibrations of the final spectra. Sample spectra are shown as figs. 1 and 2, with the ^{14}C excitation energies as compiled [10]), as seen in neutron resonance reactions [7]), or as determined from the present work.

The target thicknesses were determined by the energy loss of ^{241}Am α-particles and by careful measurements of the small-angle elastic scattering cross sections, which may be calculated reliably from the optical model. For both reactions, the absolute cross sections are determined to an overall accuracy of $\pm 8\%$.

Optical-model parameters were selected from the literature [11-13]) to describe the reactions, with adjustments of the deuteron well depths to fit the elastic data. The fits to the deuteron and ^4He elastic scattering data, on ^{13}C and ^{14}C, respectively, are shown in fig. 3. The parameters are listed in table 1. The same ^4He potential has been used for analyses of inelastic scattering on ^{13}C [ref. [12])] and ^{14}N [ref. [13])] at the 35 MeV beam energy.

Calculations were performed with the codes DWUCK4 [14]) or CHUCK2 [15]) for

† Obtained from the Atomic Energy Commission of Canada, Ltd., Chalk River, Ontario KOJ 1J0.

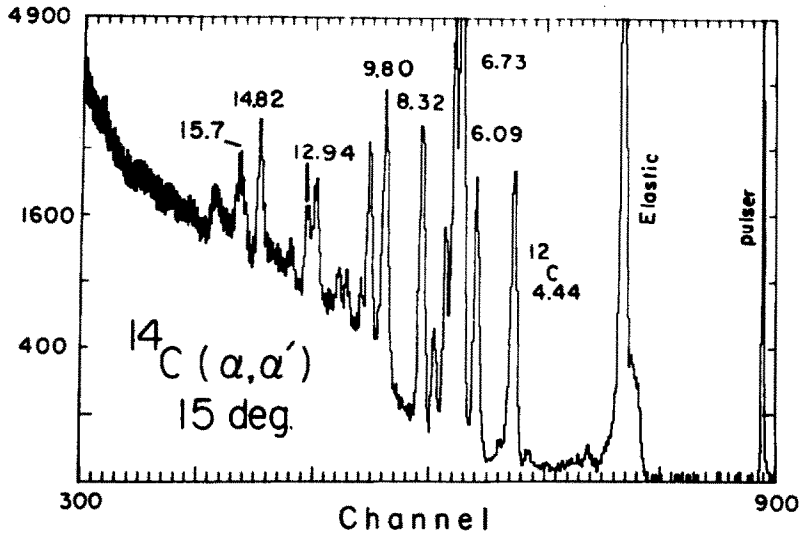

Fig. 1. A spectrum of 35 MeV ^{4}He scattered from a ^{14}C foil shows some contamination from ^{12}C. Octupole transitions are prominent at high excitations.

collective and microscopic inelastic scattering, single-step stripping and for a number of sequential processes to be described in sect. 5.

Neutron stripping to neutron bound states used the binding energy of the neutron to generate the bound wave functions, while the the method of Vincent

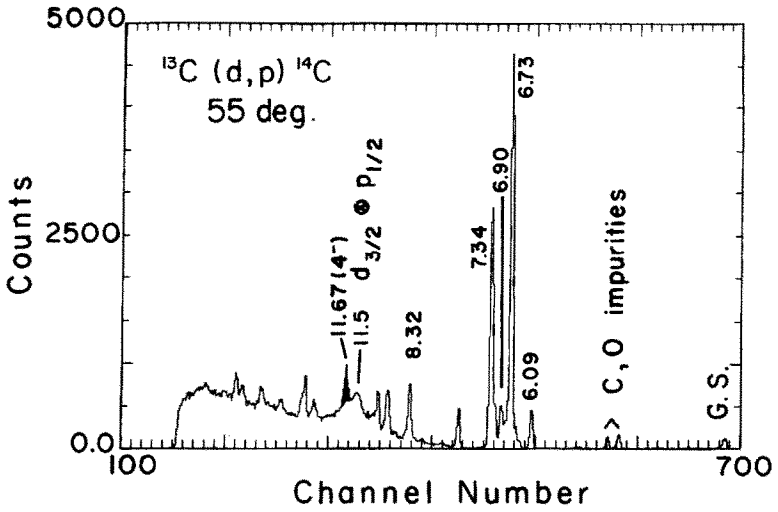

Fig. 2. A stripping spectrum to ^{14}C is shown. The ground-state peak is weak due to inefficient particle identification. A broad $d_{\frac{3}{2}}$ stripping peak is seen near 11.5 MeV.

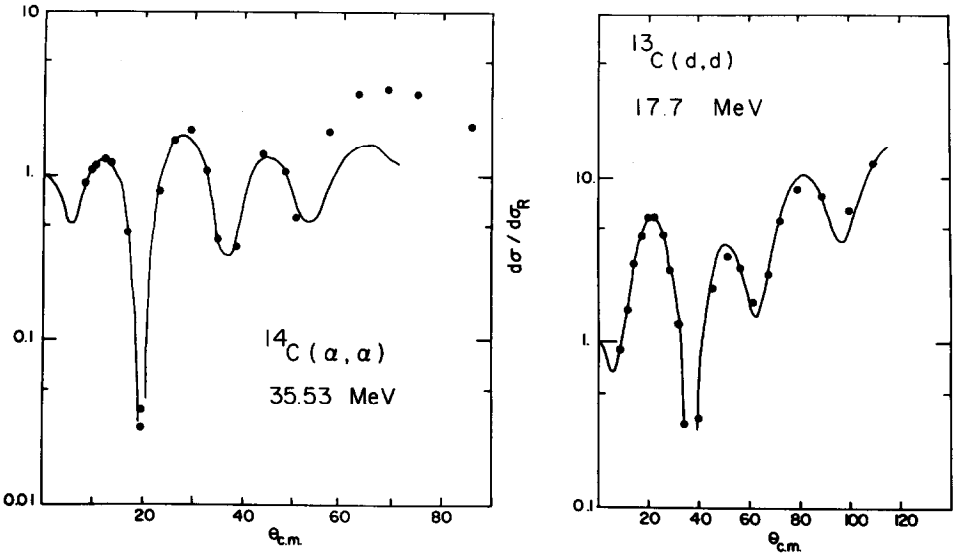

Fig. 3. Elastic-scattering data for 35 MeV ^{4}He on ^{14}C and 17.7 MeV deuterons on ^{13}C are compared to optical-model predictions using the parameters in table 1.

TABLE 1

Optical-model parameters used for DWBA and coupled-channel calculations in this work

	^{4}He [a])	Deuteron [b])	Proton [c])
V	−196.3	−111	−53.5 MeV
r_v	1.30	0.91	1.17 fm
a_v	0.635	0.88	0.75 fm
W_v	−27	0	−0.65 MeV
r_v	1.50		1.32 fm
a_v	0.52		0.56 fm
$4W_d$	0	39.2	38.9 MeV
r_d		1.75	1.32 fm
a_d		0.55	0.56 fm
$V_{s.o.}$	0	17.4	24.8 MeV
$r_{s.o.}$		0.9	1.01 fm
$a_{s.o.}$		0.9	0.75 fm
r_C	1.4	1.3	1.3 fm

Neutrons were bound in a potential of radius 1.25 fm and diffusivity 0.65 fm, with 25 times the Thomas spin-orbit strength.

[a]) Ref. [11]).

[b]) Well depths adjusted to fit the elastic data, but the other parameters are those of C. M. Perey and F. G. Perey, At. Data **17** (1976) 2.

[c]) F. D. Becchetti and G. W. Greenlees, Phys. Rev. **182** (1969) 1190.

and Fortune [16]) was used for the unbound states. This calculation also predicted the neutron widths for states of unit single-particle strength. Below 12.0 MeV the total and neutron widths are identical for ^{14}C and the observed widths and strengths may be compared to one another for each assumed angular momentum transfer. The observed and predicted angular distributions to unbound states distinguish poorly between possible angular momentum transfers.

Spectroscopic factors are defined by

$$\frac{d\sigma}{d\Omega}(\text{exp}) = 1.55S\frac{2J_f+1}{2(2j+1)}\frac{d\sigma}{d\Omega}(\text{DWBA});$$

in some cases of unknown spin we specify the assumed values of J_f and j, the final and transferred angular momenta. Use of a proton optical potential determined by a fit to ^{14}C data [17]) yielded very similar DWBA shapes and magnitudes within 10% of those predicted in the present work.

The ratio of the measured neutron width Γ to the computed width of a single-particle resonance $\Gamma_{s.p.}$ is given by [18])

$$\frac{d\sigma}{d\Omega} = \frac{\Gamma}{\Gamma_{s.p.}}(1.55)\frac{2J_f+1}{2J_i+1}\frac{d\sigma_{DW}}{d\Omega},$$

where $\Gamma_{s.p.}$ is derived from the DWBA calculation for a complete single-particle state and J_i and J_f are spins of the target and residual nuclei. All DWBA calculations were run for a presumed spin-zero target, but the proper statistical factors were used to extract the spectroscopic factors and widths for the ^{13}C target, of spin $\frac{1}{2}$.

The α-particle data were compared to collective DWBA prediction using a collective derivative form factor for $L \geqslant 2$. The isoscalar transition rates

$$B(0, L) = (2J_f+1)\langle J_f \| \sum_{i=1}^{A} r_i^L Y_L(\hat{r}_i) \| J_i \rangle^2$$

may be computed for moments of the optical potential whose derivative provides the transition form factor, using [19])

$$B(0, L) = [(\beta R)A(L+2)\langle r^{L-1}\rangle/4\pi]^2.$$

This result may be compared to the $B(C, L)$ longitudinal electron scattering result to yield the isospin content for each transition. The full complex potential was used to compute the DWBA curves for the (α, α') predictions, extract the strengths β and compute the moments. Use of the real potential alone gave moments about 1% smaller than did the full complex potential. A recent comparison of isoscalar

transition rates for the octupole excitations of ^{14}N found good agreement between measurements by 35 MeV ^{4}He and π^- and π^+ scattering[20]).

3. Positive-parity states

Positive-parity states of ^{14}C may be formed by arrangements within the 1p shell, as computed by Cohen and Kurath[21]), or by 2p2h excitations involving promotions into the sd shell as well, as computed in a weak-coupling model by Lie[22]) or by Jäger *et al.*[23]). The ^{4}He scattering results will be presented first.

The first positive-parity state is the 6.590 MeV 0^+ level. No trace of this state was seen at any angle in the α-scattering, with an upper limit of 60 μb/sr. This is less than 3% of the yield observed for the ^{12}C 7.64 MeV 0^+ level, as determined from the small ^{12}C contaminant in the target. The second excited 0^+ state at 9.746 MeV could not be resolved from the strongly excited 3^- state at 9.80 MeV in the α-spectra.

Known[7, 10]) 2^+ levels are found at 7.01, 8.32 and 10.4 MeV. The 7.01 MeV state is populated with essentially the same strength by π^+ and π^- [refs.[1, 24])], consistent with an isoscalar transition. The 8.32 MeV state is populated only by π^+ and the 10.4 MeV state mainly by π^-. Inelastic α-scattering data are shown in fig. 4, compared to collective DWBA predictions shown as the solid curves. The sole

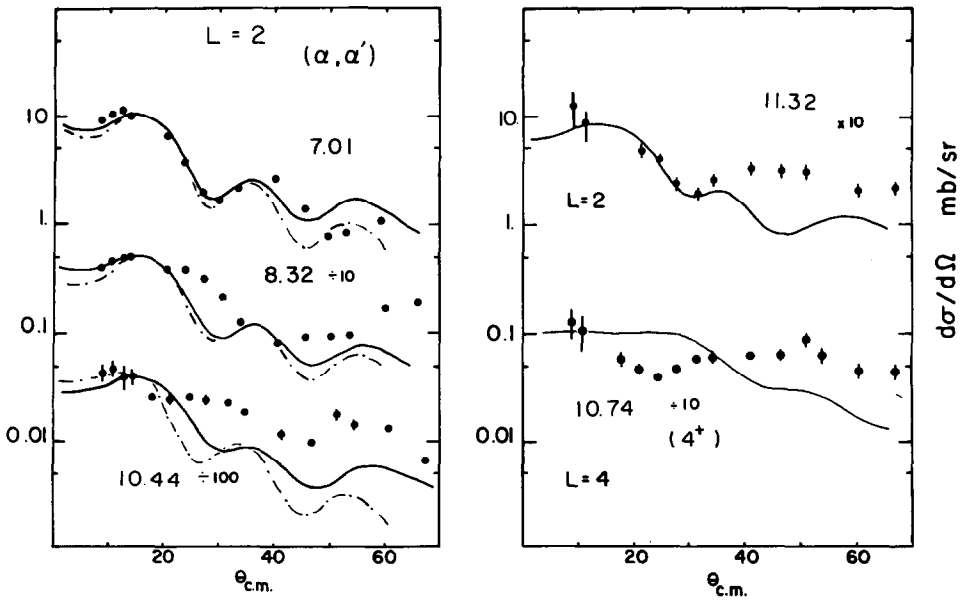

Fig. 4. Inelastic ^{4}He scattering data to 2^+ and 4^+ states of ^{14}C are compared to collective DWBA predictions as the solid curves. The 4^+ assignment for the 10.74 MeV state does not come from this fit. The microscopic DWBA predictions described in appendix A are shown as the dot-dashed curves.

TABLE 2

Collective deformations β^2 are listed for the $^{14}C(\alpha, \alpha')$ reaction, using a first-derivative form factor

State	β^2	$B(0L)$ (fm^{2L}) or EWSR
6.09 1^-	0.050	27%
6.73 3^-	0.158	6320
7.01 2^+	0.086	168
8.32 2^+	0.049	96
9.80 3^-	0.068	2720
10.45 2^+	0.038	74
10.74 4^+	0.018	
(1^-	0.014	14%)
11.32 2^+	0.014	27
12.59 3^-	0.041	1640
12.94 (3^-)	0.033	1320
13.58 1^-	0.068	92%
14.82 3^-	0.079	3160
15.66 3^-	0.096	3840
$\sum\beta_3^2$	= 0.48	for ^{14}C
	= 0.28	for ^{14}N [a])
	= 0.42	for ^{12}C [a])

For 1^- states, the fraction of the dipole sum rule [28]) exhausted is also listed. For 2^+ and 3^- states, the isoscalar reduced transition rates $B(0L)$ [ref. [19])] are listed. At the bottom are the sums of octupole strengths in several p-shell nuclei, as determined by 35 MeV α-particle inelastic scattering.

[a]) Ref. [13]).

parameter for this comparison is the deformation strength β^2, listed in table 2. Inelastic deuteron scattering [2]) to the 7.01 MeV state gave β_2^2 values between 0.04 and 0.06, smaller than observed here. Although the fit to the 7.01 MeV state is good, both the 8.32 and 10.4 MeV states are not fit well, but these two shapes are quite similar. All states are much weaker than the 21 mb/sr found for exciting the 4.44 MeV 2^+ state of ^{12}C at the same beam energy [25]).

A 2^+ assignment for a state at 11.32 ± 0.06 MeV is also made on the basis of the fit shown in fig. 4. A strong M1 transition to the 11.31 MeV 1^+ state is known [26]), but the present α-scattering data are not similar in shape to the shape seen for the 12.7 MeV 1^+ state in ^{12}C [ref. [25])]. Neutron resonance results indicate a state of spin $\geqq 2$ at 11.395 MeV [ref. [7])].

Several states are known [7, 10]) near the 2^+ level found in the (α, α') reaction at 10.44 ± 0.06 MeV. The compiled [10]) 2^+ state at 10.425 MeV has been shown to be a 3^- excitation [7]), and a $(1^+, 2^+)$ level at 10.447 MeV [ref. [7])] is identified with the state seen by (α, α'). The present (d, p) data, discussed below, for a state at 10.45 ± 0.02 MeV, of width greater than the experimental limit of 60 keV, are rather featureless, perhaps indicating the presence of unresolved states.

The calculations of Lie [22]) predict a single 4^+ state at a 9.74 MeV, entirely of 2p4h parentage and thus only accessible by inelastic scattering from the ^{14}C

ground state by sd-shell mixing. The data shown in fig. 4 are very poorly fit by the $L = 4$ DWBA prediction and only an approximate strength β_4 can be obtained.

The weak-coupling calculations of Lie[22]) predict just three 2^+ states, at 7.19, 7.43 and 9.25 MeV, while only a single low-lying 2^+ state is predicted by Cohen and Kurath[21]), at 6.83 MeV. Levels of spin 2^+ may be populated from the $\frac{1}{2}^-$ ground state of ^{13}C only by $p_{\frac{3}{2}}$ transfer, inhibited by the near closure of the $p_{\frac{3}{2}}$ shell, complete at ^{12}C in the *jj*-coupling limit. The calculations of Cohen and Kurath[21]) predict only a very weak spectroscopic factor.

In fig. 5 are shown the (d, p) data to the first two 2^+ states, compared to DWBA predictions as the solid curves. These predictions assume the $p_{\frac{3}{2}}$ neutron to be bound by its separation energy, resulting in the spectroscopic factors listed in table 3. The data to the 7.01 and 8.32 MeV 2^+ states differ greatly from one another and from the DWBA prediction. Near 20° some mechanism seems to be interfering with both transitions, with opposite sign. Sequential processes through the very strong stripping to the negative-parity states could be suspected. The third 2^+ state at 10.4 MeV is not resolved from nearby states of unknown quantum numbers; the data are shown in fig. 9.

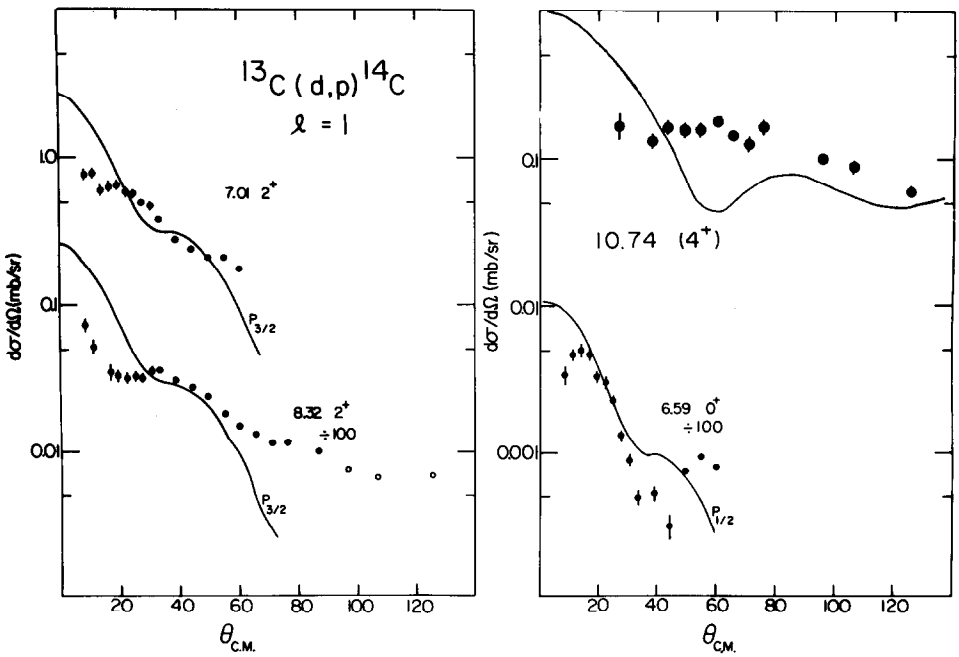

Fig. 5. Stripping angular distributions to the known positive-parity states of ^{14}C are compared to DWBA predictions for a bound final state. The $l = 1$ fits are not good and the transitions show inconsistent shapes. The 4^+ state is not expected to be populated by the $l = 3$ single stripping mechanism.

TABLE 3

Spectroscopic factors for the $^{13}C(d, p)^{14}C$ reaction are listed together with the known or assumed spin values

			Experiment		Theory			
state	J^π	j trans.	S[a])	S[b])	[c])	[d])	[e])	[f])
g.s.	0^+	$\frac{1}{2}^-$		0.59	0.44			
6.09	1^-	$\frac{1}{2}^+$	0.75	0.83		0.84	0.76	0.85
6.59	0^+	$(\frac{1}{2}^-)$	(0.14)		0			
6.73	3^-	$\frac{5}{2}^+$	0.65			0.94	0.84	0.87
6.90	0^-	$\frac{1}{2}^+$	1.02			1.00	0.96	1.00
7.01	2^+	$\frac{3}{2}^-$	0.065		0.01			
7.34	2^-	$\frac{5}{2}^+$	0.72		0.71	0.72	0.60	0.67
8.32	2^+	$\frac{3}{2}^-$	0.065		0			
9.80	3^-	$\frac{5}{2}^+$	0.07			0	0	0
10.74	4^+	$(\frac{7}{2}^-)$	(0.06)		0			
11.5	$(1^-, 2^-)$	$\frac{3}{2}^+$	~ 1					0.85

These results are compared to the DWBA results for one other experiment and to several sets of theoretical predictions. The sums of $s_{1/2}$ and $d_{5/2}$ spectroscopic factors below should be unity for stripping to empty shells.

$$\frac{1}{2J_i+1}\sum S = \begin{cases} 0.89 \text{ for } s_{1/2}, \\ 0.73 \text{ for } d_{5/2}. \end{cases}$$

[a]) Present work. [b]) Ref. [3]). [c]) Ref. [21]).
[d]) Ref. [22]). [e]) Ref. [31]). [f]) Ref. [23]).

The 1^+ state at 11.31 MeV [ref. [26])] could be populated by $l = 1$ stripping, but this region of the spectrum was obscured by a strong, broad $d_{\frac{3}{2}}$ stripping peak.

The thin front detector of our telescope proved to yield unreliable proton identification for the ground state of ^{14}C, but a reliable spectroscopic factor for this transition is available from other data [3]). The present data for the 6.59 MeV 0^+ state are compared to the $p_{\frac{1}{2}}$ DWBA prediction in fig. 5; the fit is very bad, indicating an inadequate description of the reaction mechanism. The fit shown yields a spectroscopic factor $S = 0.14$, compared to an average of 2.35 for the ground state [3]). An analysis of $^{12}C(t, p)^{14}C$ data [27]) to these 0^+ states indicates a ratio of 7.2 for the (d, p) spectroscopic factors, due to mixing of p-shell and sd-shell configurations. Given the poor quality of the stripping fit for the 6.59 MeV data, the present results may be regarded as agreeing with this picture.

The stripping data to the 10.74 MeV 4^+ state are compared to an $f_{\frac{7}{2}}$ (bound) DWBA prediction in fig. 5. The rather featureless data are not reproduced by the calculation, and only a rough spectroscopic factor is provided in table 3. This 4^+ state has but little 1p1h amplitude.

Tables 2 and 3 show the results of the present work for the even parity states of

^{14}C. Deformations β and isoscalar reduced transition rates are given for the (α, α') reaction and neutron spectroscopic factors are listed together with the assumed spins.

Mixing of p-shell and sd-shell configurations for the 2^+ states of ^{14}C will have important consequences for the microscopic DWBA predictions for inelastic scattering. An analysis of several 2^+ states will be found in appendix A.

4. Negative-parity levels of ^{14}C

No (α, α') yield for the 6.902 MeV 0^- level was detected, as expected by parity considerations for the scattering of a spin-zero projectile. Data for scattering to the 7.34 MeV 2^- and 11.37 MeV 4^- states will be treated in sect. 5, where multistep processes will be considered.

The α-scattering data for the first excited 1^- state at 6.09 MeV are compared in fig. 6 to a solid curve computed for a form factor taken as the first derivative of the optical potential. The characteristic shape allows a further 1^- assignment to a state at 13.58 MeV. The known 1^- state at 9.806 MeV [ref. [7])] would be obscured by the strong 9.83 MeV 3^- excitation. The strengths β_1^2 from this analysis are listed in table 2, but are difficult to relate to a collective model.

Use of the form factor of Harakeh and Dieperink [28]) allows the isoscalar dipole strength to be compared to a sum rule. The form factor, described in detail elsewhere [28]), is

$$\text{f.f.} = -\frac{\beta}{R\sqrt{3}}\left[3r^2\frac{\mathrm{d}}{\mathrm{d}r} + 10r - \tfrac{5}{3}\langle r^2\rangle\frac{\mathrm{d}}{\mathrm{d}r} + \varepsilon\left(r\frac{\mathrm{d}^2}{\mathrm{d}r^2} + 4\frac{\mathrm{d}}{\mathrm{d}r}\right)\right]U(r).$$

The second derivative term was found to always be less than 1% of the form factor and was ignored. The strength β obtained from comparison of the data to the DWBA prediction may be compared to the sum-rule limit of

$$[\beta R(100\%)]^2 = \frac{6\pi\hbar^2R^4}{MAE}[11\langle r^4\rangle - \tfrac{25}{3}\langle r^2\rangle^2 - 10\varepsilon\langle r^2\rangle]^{-1}.$$

The radial moments of the real and imaginary optical potentials are nearly identical. The broken curve in fig. 6 compared to the 6.09 MeV 1^- data as the open points shows the fit with this Harakeh and Dieperink form factor, exhausting $(30^{+9}_{-5})\%$ of the sum-rule limit, with uncertainties taken from the extreme credible fits to the forward-angle data. The calculation did not include Coulomb excitation, which was found to destroy the good forward-angle fit when included. This isoscalar dipole strength is much greater than the 4.2% reported [28]) for ^{16}O, and represents a truly collective excitation. Just the same cross section is found for

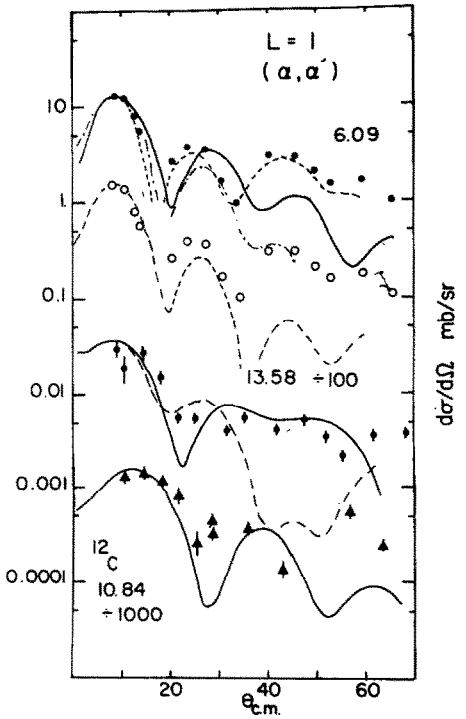

Fig. 6. Inelastic scattering data to 1^- states are shown, including the 10.84 MeV state of ^{12}C. The solid lines show DWBA predictions with a simple derivative form factor. The broken curve through the top solid data points represents the $^{13}C(\alpha, \alpha')$ data to the lowest $\frac{1}{2}^+$ state [12]) and the dot-dash curve shows the microscopic DWBA prediction. The open points repeat the 6.09 MeV data, scaled down by a factor of ten. The broken curve through these points and through the 13.58 MeV data shows the DWBA calculation using the form factor of Harakeh and Dieperink [28]).

(α, α') excitation of the first $\frac{1}{2}^+$ state in ^{13}C [ref. [12])], as shown by the broken curve in fig. 6 compared to the solid data points.

A weaker $L = 1$ cross section is found at 13.58 MeV. The small-angle rise is a sure indicator of the spin, as emphasized by comparison to the α-scattering data for the 10.84 MeV 1^- state of ^{12}C, also shown in fig. 6. The ^{12}C transition also exhausts 30% of the isoscalar dipole sum rule, with a lower cross section at a higher excitation than in ^{14}C. The prediction using the form factor of Harakeh and Dieperink is shown as the broken curve for the 13.58 MeV transition.

The 13.58 MeV state of ^{14}C is important for the energy-weighted nature of the isoscalar dipole sum rule, and exhausts 92% of that sum rule. The forward-angle data points are vital in the spin assignment for this very collective state. Examination of these transitions by higher-energy α-particle scattering would be most valuable to verify the exhaustion of the isoscalar dipole sum rule strength in ^{14}C. It is worth noting that a calculation on the dipole properties of ^{18}O used a

^{14}C core for the α-particle molecular structure [29]). The level ordering in ^{14}C is, however, not as expected for the proposed model.

Shell-model calculations predict three 1^- states in ^{14}C, at 6.78, 9.23 and 10.75 MeV [ref. [22])] or at 5.46, 8.79 and 11.45 MeV [ref. [22])]. More than this number of dipole states are known [7]).

An unexpected forward-angle rise is found for the α-scattering to the 10.74 MeV 4^+ state, as seen in fig. 4. If this were interpreted as due to a 1^- excitation another 14% of the sum strength would be exhausted. Since the DWBA fit is poor and no such sharp state is known [7]), no conclusion can be drawn.

At 35 MeV, the (α, α') reaction has proven to be very effective at locating octupole excitations. Data for known and newly assigned transitions are compared to collective DWBA predictions in fig. 7. The transition strengths β_3^2 are listed in table 2. The poorly justified 3^- assignment to the 12.58 MeV peak may be identified with the known 3^- state at 12.61 MeV [ref. [30])]. The poor fit to the 12.94 state allows only a tentative new 3^- assignment, although the state is seen in neutron resonance reactions [7]).

Only two 3^- states are predicted, at 5.72 and 9.02 MeV [ref. [22])], compared to the total of six found by (α, α') in this work. This excess of octupole transition was also noted in ^{14}N [ref. [13])], and shows more extensive involvement with the sd shell than is found in current calculations.

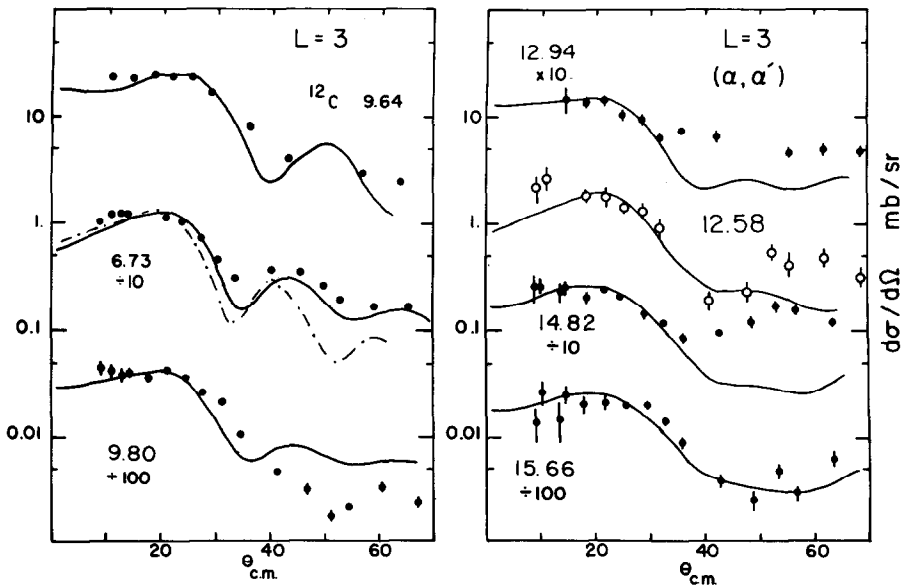

Fig. 7. Data for $L = 3$ excitations in ^{14}C are compared to collective DWBA predictions shown as the solid curves. The dot-dash line for the 6.73 MeV state represents the microscopic DWBA prediction. Data for the strong 3^- state in ^{12}C are also shown, compared to the same collective prediction for that target.

The octupole isoscalar reduced transition rates $B(03)$ are also listed in table 2. For ^{14}N, α-scattering results have been found to agree with inelastic pion-scattering data [20]).

The sum of isoscalar octupole strengths β_3^2 in ^{14}C is as great as for the single 9.64 MeV 3^- state in ^{12}C, and greater than the summed strength found in an equivalent excitation span in ^{14}N. These sums are compared in table 2.

A microscopic shell-model DWBA analysis of several negative-parity states of ^{14}C populated by the α-particle scattering is presented in appendix A. A comparison of isoscalar and electromagnetic transition rates for the 6.73 MeV 3^- state is located in appendix B.

The shell-model structures of the negative-parity states of ^{14}C are sensitively probed by the (d, p) results, requiring $l = 0$ or $l = 2$ transfers. The data are compared to DWBA predictions in fig. 8, with the resulting spectroscopic factors listed in table 3, together with several sets of predicted spectroscopic factors [22, 23, 31]).

The deep minimum for the 6.09 1^- transition places a limit on the $d_{\frac{1}{2}}$ component of that state. Some slight excess over the shape found for the 0^- state places a limit of 0.03 on the $(\frac{1}{2}^- \times \frac{3}{2}^+)$ spectroscopic factor for this state. Predicted amplitudes [23]) provide an estimate of 0.022 of the $s_{\frac{1}{2}}$ spectroscopic factor, or 0.016 for the $d_{\frac{1}{2}}$ strength.

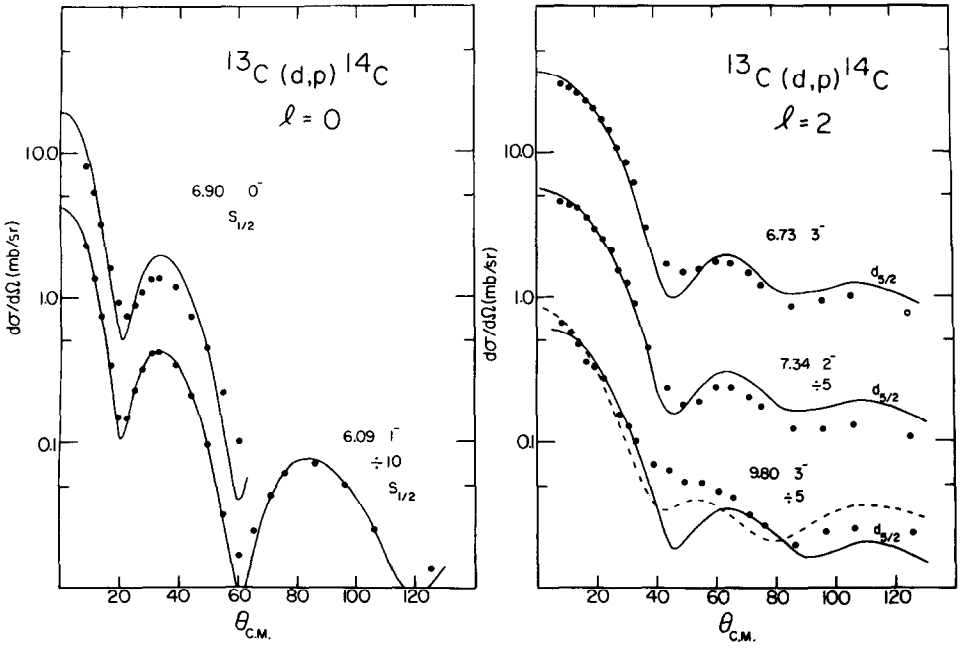

Fig. 8. Stripping data to known odd-parity states of ^{14}C are compred to DWBA predictions for bound final states. The effect of a coherent multistep contribution is shown as the broken curve for the 9.80 MeV state, as described in the text.

Very good fits for the two $l = 0$ transitions are found, and the forward-angle data are used to normalize to the DWBA for the spectroscopic factors. The present result for the 1^- state at 6.09 MeV is very near that previously measured [3]) and is in agreement with three predicted results. The three predictions for the $s_{\frac{1}{2}}$ strength to the 6.90 MeV 0^- state are are also in good agreement with one another and with the present data. Almost all of the $s_{\frac{1}{2}}$ single-particle strength is found in these two transitions.

The strong $d_{\frac{5}{2}}$ transitions are to the lowest 3^- and 2^- states. The 2^- spectroscopic factors are very close to those predicted and previously measured, but the 3^- result seems significantly less than predicted, as seen in table 3. The solid curve for the $d_{\frac{5}{2}}$ neutron stripping to the 9.80 MeV state (fig. 8) confirms the 3^- assignment from the scattering result. The dashed curve for this state is the result of a CHUCK calculation including the two-step configuration $(2^+ \times s_{\frac{1}{2}})$ in addition to the single-step $d_{\frac{5}{2}}$ transfer. Both calculations use a weak $d_{\frac{5}{2}}$ spectroscopic factor of 0.07. The two-step path used $\beta_2^2 = 0.086$ and a unit $s_{\frac{1}{2}}$ spectroscopic factor. This process somewhat improves the quality of the fit, but does not change the conclusion for the magnitude of the $d_{\frac{5}{2}}$ stripping spectroscopic factor.

Data for stripping to the 12.58 MeV 3^- state [30]) are compared to the required $d_{\frac{5}{2}}$ unbound DWBA prediction in fig. 9, and a good fit is found.

A very strong and broad stripping peak at 11.5 MeV corresponds exactly in Q-value, width and strength to the $d_{\frac{5}{2}}$ stripping [18]) on ^{12}C, as seen in comparison spectra taken during the present work. The data are shown in fig. 9, compared to the DWBA prediction for $d_{\frac{5}{2}}$ stripping to a state unbound by the experimental positive binding energy. A unit spectroscopic factor fits the magnitude of the data, but the observed width is only about one third of that predicted for a single-particle state. The smooth shape of the peak indicates that the 1^- and 2^- states formed by the coupling of the $d_{\frac{5}{2}}$ neutron to the ^{13}C $\frac{1}{2}^-$ ground state are separated by much less than their widths. The sum of the 1^- and 2^- spectroscopic strengths estimated from predicted amplitudes is 0.85 [ref. [23])].

5. The 11.7 MeV 4^- state

An important feature of ^{14}C is the great isospin asymmetry noted for the 11.7 MeV 4^- state, populated not at all by π^+ inelastic scattering [1]).

The excitation energy of the 4^- state is found to be 11.72 MeV in electron scattering [9]) and one (5^-) state is compiled at 11.73 ± 0.01 MeV, another at 11.67 ± 0.01 MeV [ref. [10])]. The weak peak seen in the present ^4He scattering lies at 11.62 ± 0.08 MeV, and possibly corresponds to the state other than that seen in electron scattering. The neutron stripping peak treated here is at 11.67 ± 0.04 MeV. The existence of two high-spin states of close separation lead to the uncertainties in the analysis. A 4^- state will be assumed here.

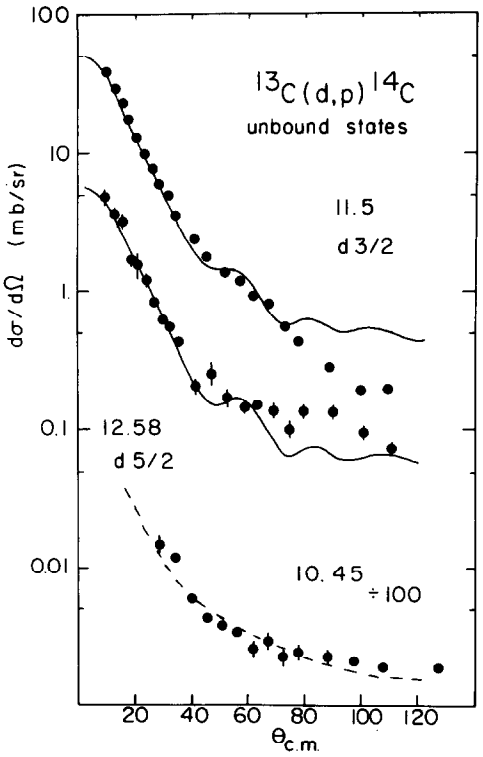

Fig. 9. Stripping data to unbound states of ^{14}C are compared to the appropriate DWBA calculations as the solid curves. Data to the unresolved states near 10.44 MeV are compared to the shape found for the $^{12}C(d, p)^{13}C$ transition to the 10.75 MeV $\frac{7}{2}^-$ state, shown as the broken curve.

The simple stretched nature of the expected configuration, $(p_{\frac{3}{2}}^{-1}d_{\frac{5}{2}})$, enables us to compute two-step probabilities for exciting this state although no single-step mechanism is available to either reaction reported here. There calulations are similar to those reported [12,32]) for the $\frac{9}{2}^+$ state of ^{13}N, also of stretched nature. Only a single 4^- state is predicted by weak-coupling calculations [22,23]), but at least one more is known at 17.26 MeV [ref. [1])].

In addition to the 4^- yield from inelastic α-scattering, fig. 10 shows the 2^- cross sections for the 7.34 MeV state of ^{14}C and the 11.83 MeV state of ^{12}C, since two-step models should consistently account for both spin transfers. The shape and magnitude of the ^{12}C and ^{14}C 2^- excitations are identical, providing a strong clue as to the reaction mechanism.

A sequential nucleon transfer path to the 4^- and 2^- states would allow inelastic excitation with $(\alpha, t)(t, \alpha)$, to a $\frac{5}{2}^+$ state of ^{15}N followed by $p_{\frac{3}{2}}$ pickup. Two step calculations with CHUCK gave yields many orders of magnitude weaker than the data, a consequence of the large momentum transfer, occurring twice in the reaction. This path may be neglected.

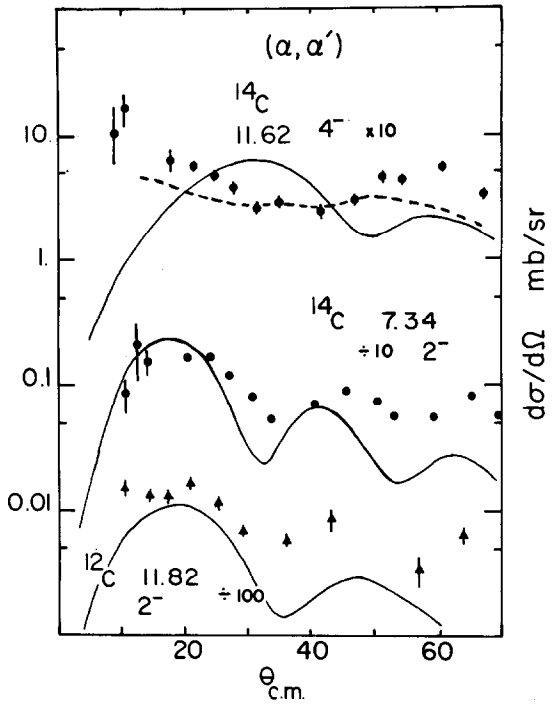

Fig. 10. Data for α-scattering to the 2^- and 4^- states of ^{14}C are shown together with points for exciting the first 2^- state of ^{12}C. The broken curve shows the data for the $\frac{9}{2}^+$ state of ^{13}C, multiplied by $\frac{9}{20}$. Solid curves represent the sequential β_2 β_3 excitations, without free parameters, as described in the text.

Sequential scattering through the known strong β_2 and β_3 strengths is a more reasonable process. The solid curve for the 2^- state of ^{12}C is the result of such a calculation. The first 3^- state is taken to be of equally mixed axial quantum projections $K = 0^-$ and 2^-, with $\beta_3 = 0.74$ to reproduce the data. The β_2 deformation of the negative-parity band is taken in the rotational model from the spacing of the unmixed 2^- and 4^- $T = 0$ states, and is equal to 0.90. The strong coupling Clebsch-Gordan coefficients govern the yield to the final states, only from the $K = 2^-$ part of the 3^- level. This calculation roughly accounts for the shape and magnitude of the 2^- data in ^{12}C.

For ^{14}C a similar calculation was performed, with $\beta_3 = 0.40$ (see table 2) and $\beta_2 = 1.34$, taken from the band spacings. The negative-parity configuration is even more deformed in ^{14}C than in ^{12}C, although the ^{12}C ground-state band is so apparent. The solid curve representing this calculation accounts well for the ^{14}C 2^- data in fig. 10.

The 4^- state may have its parentage in the ^{13}C $\frac{9}{2}^+$ state at 9.50 MeV. In fig. 10 is shown a broken curve representing $\frac{9}{20}$ of the α-scattering data for that state in

^{13}C [ref.[12])]. The good fit confirms the expected parentage, using the statistical weights with the known spins.

Sequential scattering computed as for the 2^- state yields the parameter-free solid curve compared to the 4^- data in fig. 10. Although the shape is not matched to the data, the magnitude is roughly correct.

The unnatural parity of the supposed 4^- state at 11.67 MeV places a strong constraint on the α-particle scattering. Conservation of parity and angular momentum for the spin-zero projectile are sufficient to preclude any zero-degree cross section for unnatural-parity states[33]). This is as observed for the 7.34 MeV 2^- state and is independent of the reaction mechanism itself. The 11.6 MeV data do not seem to be consistent with a zero-degree minimum, indicating a natural parity for this state, inconsistent with spectroscopic models used for the pion scattering. Further detailed studies of the spin of this state are called for, especially in light of possible confusion between two high-spin states of small energy separation and possibly similar parentage.

The stripping data for the 4^- state are shown as the broken curve in fig. 11 and

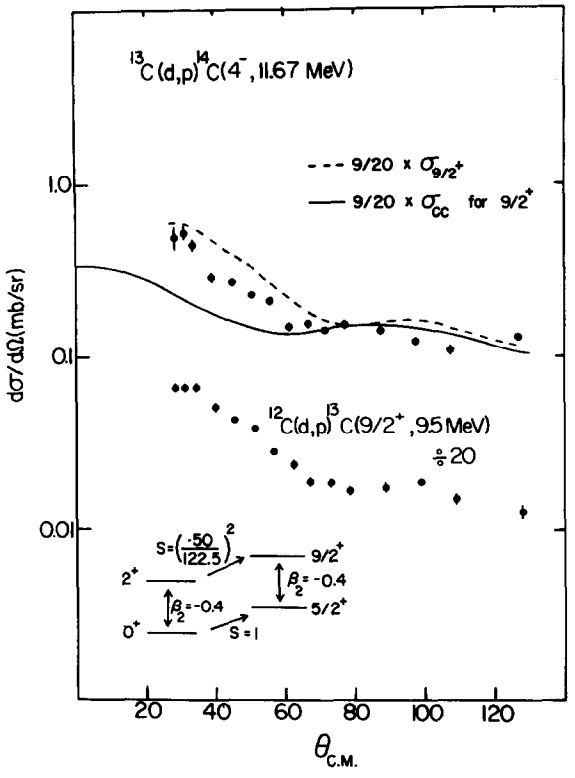

Fig. 11. Data for multistep stripping to the $\frac{9}{2}^+$ sate of ^{13}C and the 11.67 MeV state of ^{14}C are shown. The broken curve represents two-step paths shown provide the solid curve, as described in the text.

compared to those for the $^{12}C(d, p)^{13}C$ reaction to the 9.5 MeV, $\frac{9}{2}^+$ state, as measured in the present work.

This curve represents $\frac{9}{20}$ of the stripping cross section to the $\frac{9}{2}^+$ state, as expected for a 4^- state with full parentage in the ^{13}C $\frac{9}{2}^+$ state. The strong similarity in the angular distributions and the well-matched magnitude support the idea of the weak-coupling picture. Neither reaction to the $\frac{9}{2}^+$ or 4^- state can proceed by a single-step process, since the $g_{\frac{9}{2}}$ states are expected at $2\hbar\omega$ (near 35 MeV). The stripping calculations to ^{14}C are taken to be $\frac{9}{20}$ of the result computed for a spin-zero target of ^{12}C. Two two-step sequential paths, $d_{\frac{5}{2}}$ stripping onto the 2^+ collective state of ^{12}C and $d_{\frac{5}{2}}$ stripping to the strong $\frac{5}{2}^+$ (3.85 MeV) state of ^{13}C followed by the collective quadrupole excitation to the $\frac{9}{2}^+$ state, are expected to be equally important for ^{13}C. Both paths are schematically shown in fig. 11, along with the phases and strenngth parameters of the amplitudes used in the two-step CCBA (coupled-channel Born approximation) calculation. [A very similar calculation was reported[32]) for proton stripping to the $\frac{9}{2}^+$ state of ^{13}N.] This calculation was done with the code CHUCK[15]) and the optical parameters used are summarized in table 1. The β_2 value of the ^{12}C quadrupole excitation and the spectroscopic factor for stripping to the $\frac{5}{2}^+$ (3.85 MeV) state were derived from $^{12}C(d, d')$ [ref.[2])] and $^{12}C(d, p)$ data[18]). The same strengths were adopted for the opposite path.

The solid curve in fig. 11 represents $\frac{9}{20}$ of the above calculation, using only statistical weighting factors with the known spin values. The angular distribution is not accounted for very well, but the magnitudes of the cross sections are reasonably reproduced. The result of the calculation varies somewhat with the optical parameters and the various features of the calculation, however, this sensitivity does not change our understanding significantly.

6. Conclusions

Two reactions specific to the isospin and neutron structures of several levels of ^{14}C have been examined. A number of new spin assignments are made; of special importance are the collective 3^- states. Data-to-data comparisons between states in ^{14}C and ^{13}C demonstrate the parentage of the important states. Sequential reaction processes account fairly well for the excitation of the 4^- state in both (d, p) and (α, α'), while success is also found for sequential α-excitation of the 2^- states in ^{12}C and ^{14}C. The absolute isoscalar transition strengths for ^{14}C will be of great value when absolute pion reaction amplitudes become available, since the isoscalar amplitudes will be a constraint to select the proper root in extracting isospin amplitudes from the pion data, permitting advances in the isovector spectroscopy in the p-shell. Isoscalar dipole transitions exhausting much of the sum rule are found, indicating truly collective modes not previously seen.

The complementary nature of the reactions used for the present study of ^{14}C will serve to constrain theories on the isospin nature of the levels of this nucleus, mixing its particle and hole or neutron and proton structures. Appendix B examines some of the isospin relations among the data for ^{14}C.

We wish to thank M. A. Rumore, R. S. Raymond, J. L. Ullmann and Y. Yasue for assistance in taking the data. Mr. J. L. Gallant of the Chalk River Laboratories prepared an excellent ^{14}C foil for this experiment.

Appendix A

MICROSCOPIC FORM FACTORS FOR (α, α')

Mixing of the p-shell and sd-shell configurations provides form factors for inelastic scattering with nodes that may appear in the important surface region. Microscopic inelastic α-particle scattering form factors for $L=1$ and $L=3$ excitations in ^{9}Be have been given in ref. [34]), and here are applied to ^{14}C. The dot-dash microscopic DWBA curve for the 6.73 MeV 3^- state in fig. 7 shows fair agreement with the data. This transition has a nodeless form factor, so the shape is determined by the range and size parameters. The fit in fig. 7 uses an oscillator length parameter a of 1.73 fm [ref. [35])] and a gaussian Nα inverse range [36]) γ of 0.442 fm^{-1}.

The wave functions of Lie [22]) indicate that the ^{14}C quadrupole excitations from the ground state among the p-shell holes and among the sd shell particles will be constructive for the 7.01 MeV state and destructive for the 8.32 MeV state. This may explain the unusual angular distribution for the latter state seen in fig. 4.

The microscopic model for inelastic α-scattering [34]) may be extended to quadrupole excitations, yielding radial transition matrix elements for hole and particle states in the d- and s-shells:

$$(\mathrm{hh}) = 4\pi V_0 \sqrt{\frac{21}{8\pi}}\left[\frac{16}{3ba^5} + \frac{\gamma^4}{8b^6}r^2\right]\exp\left[-r^2(\gamma^2 - \gamma^4/b^2)\right],$$

$$(\mathrm{dd}) = 4\pi V_0 \sqrt{\frac{2}{7\pi}}\left[\frac{14\gamma^4 r^2}{15a^7b^9} + \frac{4\gamma^8 r^4}{15a^7b^{11}}\right]\exp\left[-r^2(\gamma^2 - \gamma^4/b^2)\right],$$

$$(\mathrm{ds}) = -4\pi V_0 \sqrt{\frac{9}{10\pi}}\left[\left(\frac{7\gamma^4}{3a^9b^9} - \frac{\gamma^4}{a^7b^7}\right)r^2 + \frac{2\gamma^8 r^4}{a^7b^{11}}\right]\exp\left[-r^2(\gamma^2 - \gamma^4/b^2)\right.$$

with $b^2 = \gamma^2 + 1/a^2$. Since the $s_{\frac{1}{2}}$ and $d_{\frac{5}{2}}$ orbits are nearly degenerate, the particle excitation (pp) is taken to be comprised equally of the (dd) and (ds) forms, $(\mathrm{pp}) = \sqrt{\frac{1}{2}}\,(\mathrm{dd} + \mathrm{ds})$. Since there is a node when combining the sd and dd terms, it

is necessary to perform DWBA calculations to compare the yields to the three 2^+ states, with form factors [22]) as

$$\langle \text{g.s.}|2_1^+\rangle = 0.811\,(\text{hh}) + 0.106\,(\text{pp}),$$
$$\langle \text{g.s.}|2_2^+\rangle = 0.66\ \ (\text{hh}) - 0.122\,(\text{pp}),$$
$$\langle \text{g.s.}|2_3^+\rangle = 0.166\,(\text{hh}),$$

remembering that one-body scattering cannot connect the 2p and 2h excitations.

Since the p-shell (hh) excitation is proton-like, and the sd shell (pp) excitations are approximately symmetric between neutrons and protons, their same interference has been applied to the isospin asymmetries seen in the pion scattering [1]). Square root signs were omitted for the parameters α_0 and β_0 in ref. [1]), and a different phase convention is used, but the form factors may be compared. The mixing of the p-shell and sd-shell excitations is much less in the present work than was used in ref. [1]).

The shapes of the $L = 2$ microscopic predictions are shown as the dot-dash curves adjusted and compared to the data in fig. 4. The predicted ratios of magnitudes for the three 2^+ states are

$$7.01 : 8.32 : 10.44 = 1 : 0.32 : 0.026,$$

compared to the observed 1 : 0.57 : 0.44. Although the relative strength of the 8.32 MeV state is within a factor of two of the predictions, the third 2^+ state of ^{14}C is much more strongly excited than provided for in this model, where it is predominantly 2p4h in nature. This could point to greater sd-shell admixture in the ^{14}C ground state, but recent data [37]) indicate little core excitation in the ^{14}C target.

As expected for the strongly absorbed projectile, the shapes of the microscopic predictions differ but little from the collective shapes. The only node, for the 8.32 MeV state, lies at 12.25 fm, too far out to have much influence. The microscopic prediction differs the most from the collective shape for the third 2^+ state, but is in worse agreement with the data. The use of harmonic-oscillator radial wave functions is not correct for this very unbound state.

The collective DWBA shape (the solid curve) fits the 6.73 MeV 3^- data in fig. 7 more closely than does the shell-model prediction, but neither the first derivative collective or shell-model $L = 1$ curves fit the 6.09 MeV 1^- data well. The dot-dash $L = 1$ curve in fig. 6 is sensitive to the parameters of the prediction, since the form factor has a node at 5.45 fm. The broken curve in fig. 6 shows the data for the 3.09 MeV $\frac{1}{2}^+$ excitation in ^{13}C by α-scattering at the same energy, in good agreement with the 6.09 MeV data for ^{14}C, shown as the solid data points.

Volume integrals of the strength of the αN potential are more than twice as

great for the 3^- fit compared to the 1^- fit, reflecting the higher octupole collectivity. Volume integrals are 2.7×10^4 MeV·fm^3 for the 6.73 MeV 3^- state and 1.2×10^4 MeV·fm^3 for the 6.09 MeV 1^- state. In ^{9}Be, the volume integral required for an $L = 3$ transition was 3.1×10^4 MeV·fm^3, while values from 2.2×10^4 to 5.2×10^4 are required for $L = 1$ transitions.

Three terms enter the Millener and Kurath 1^- state wave functions [31]), and unless these are correct the shape of the (α, α') DWBA prediction will be altered sensitively; only the $p_{\frac{1}{2}}{}^{-1} s_{\frac{1}{2}}$ excitation was considered. Due to the neutron excess, the spurious c.m. motion is not removed from this simple calculation, nor from the calculations reported for ^{9}Be in ref. [34]).

Appendix B

ISOSPIN CONTENT OF 2^+ AND 3^- TRANSITIONS

The present reduced isoscalar transition rates $B(02)$ and the electromagnetic longitudinal $B(C2)$ allow the separation of the isoscalar and isovector amplitudes [38]) for the quadrupole excitations of the two lower 2^+ state of ^{14}C. A convenient parameterization is to use the deformation lengths, related by

$$A\beta R_0 = N\beta R_n + Z\beta R_p,$$
$$(N-Z)\beta R_1 = N\beta R_n - Z\beta R_p,$$

with subscripts for isoscalar/isovector or neutron/proton. These lengths are proportional to the square roots of the reduced transition rates, normalized to the number of participants in the collective motion:

$$\beta R_0 \propto (B(02)/A^2)^{\frac{1}{2}},$$
$$\beta R_p \propto_I (B(C2)/Z^2e^2)^{\frac{1}{2}}.$$

The ratio of isovector to isoscalar strengths is defined as

$$x = \sqrt{\frac{T}{T+1}}\,\frac{N-Z}{A}\,\frac{\beta R_1}{\beta R_0},$$

with the first term from the isovector excitation of a state of isospin T from the ground state of the same isospin, $T = 1$, for ^{14}C. For a collective vibration of all nucleons together, $\beta R_1 = \beta R_0$ and $x = 0.101$. In terms of the present experimental results,

$$\left|\frac{\beta R_0}{\beta R_p}\right| = \pm\left(\frac{B(02)}{B(C2)}\right)^{\frac{1}{2}}\frac{Ze}{A} = \frac{\pm 12}{14(1-\sqrt{2}x)}.$$

The $B(C2)$ values used are $4.1 \pm 1.5\ e^2 \cdot fm^4$ for the 8.32 MeV state[39]) and $18.5 \pm 2 e^2 \cdot fm^4$ from the average of lifetime[10]) and electron scattering[39]) results for the 7.01 MeV 2^+ state. For the 7.01 MeV state, the two roots are $x_+ = 0.24$ and $x_- = 1.18$, while for the 8.32 MeV state, $x_+ = 0.42$ and $x_- = 1.00$. These results and their uncertainties are gathered in table 4. The positive root for the 7.01 MeV state is near that of the collective vibration, 0.10. A test of the simple isospin relations (and the assumption of collective form factors) is provided by comparing these isospin ratios to the asymmetries seen in pion scattering:

$$A_\pi = \frac{d\sigma(\pi^-) - d\sigma(\pi^+)}{d\sigma(\pi^-) + d\sigma(\pi^+)}.$$

Under the assumption at similar distortions, $d\sigma/d\Omega \propto (\beta R)^2$. Then, in terms of the isospin ratio x,

$$A_\pi = \frac{4x(5Z^2 + 6NZ + 5N^2) - 4(x^2+4)(N^2 - Z^2)}{(x^2+4)(5Z^2 + 6NZ + 5N^2) - 16x(N^2 - Z^2)}.$$

For the 7.01 MeV state, the positive root predicts an asymmetry near that observed[1]), probably within the uncertainty required by the lack of consideration of differences in the distortions for π^+ and π^-. For the 8.32 MeV state, even the sign is wrongly predicted for A_π. Since the ratio of the α-scattering reduced transition rates for the 8.32 MeV state to the 7.01 MeV state (0.57) is greater than that for electron scattering (0.22), the transition must be neutron-like. The pion data require a proton-like transition[1]).

This discrepancy is based on a collective model, used as the form factor in all α-

TABLE 4

The longitudinal electromagnetic $B(CL)$ and isoscalar $B(0L)$ reduced transition rates are used to determine the ratio x of isovector to isoscalar strength and to predict pion scattering asymmetries for three states of ^{14}C

State	Positive root	Negative root
$6.73(3^-)$	$x = 0.35 \pm 0.05$	$x = 1.06 \pm 0.15$
	$A_\pi = 0.21 \pm 0.05$	$A_\pi = 0.78^{+0.07}_{-0.10}$
$7.01(2^+)$	$x = 0.24^{+0.08}_{-0.13}$	$x = 1.18^{+0.12}_{-0.08}$
	$A_\pi = 0.096^{+0.08}_{-0.07}$	$A_\pi = 0.84 \pm 0.05$
		$A_\pi(\text{exp})^a) = -0.06 \pm 0.03$
$8.32(2^+)$	$x = 0.42^{+0.08}_{-0.17}$	$x = 1.00^{+0.17}_{-0.08}$
	$A_\pi = 0.27^{+0.07}_{-0.17}$	$A_\pi = 0.74^{+0.07}_{-0.05}$
		$A_\pi(\text{exp})^a) = -0.96^{+0.04}_{-0.10}$

a) Ref.[1]).

particle, electron and pion analyses. The only support, other than convenience, for this model is the close similarity of the transition radii seen in electron scattering to the two states [39]. The 8.32 MeV state is unbound to neutron decay, providing a long radial tail for the neutron wave function, sampled differently by the α-particle and electron. If significant, this effect must negate the simple ratio arguments of this appendix. The strong role of binding energy effects on transition rates has recently been noted for several p-shell nuclei [40], and close correspondences between the excitation energies of charge asymmetric states and thresholds for nucleon decays have also been noted [41].

The isospin structure may be determined for the lowest 3^- (6.73 MeV) state by comparing isoscalar and electromagnetic reduced transition rates. The observed lifetime and branching ratio [42]) yield $B(C3)\uparrow = 395 \pm 70\, e^2 \cdot \mathrm{fm}^6$, or 2.33 ± 0.27 single-particle units. For a bulk vibrational excitation, the isoscalar $B(03)$ should be equal to $(N/Ze)^2$ times this $B(C3)$ [ref. [19])], or 2150 ± 380 fm^6. This is far below the observed value of 6320 fm^6, listed in table 2.

The isospin strength ratio x and the resulting pion asymmetry predictions are presented in table 4. The positive root is nearer the collective expectation of $x = 0.10$, but still predicts some neutron-like asymmetry. In these predictions, the uncertainty estimates are based on the quoted accuracy of the electromagnetic results and a 10% uncertainty in the α-particle results; this underestimates the uncertainty due to the necessary radial moment calculation.

For light nuclei such as ^{14}C, the double-folding treatment of density-dependent NN interactions has been shown to remove discrepancies between isoscalar rates determined by α-scattering and electromagnetic probes [43]). This treatment may resolve the discrepancy between the results for the 6.73 MeV 3^- state.

References

1) D. B. Holtkamp *et al.*, Phys. Rev. Lett. **47** (1981) 216
2) F. E. Cecil *et al.*, Nucl. Phys. **A255** (1975) 243
3) S. K. Datta, G. P. A. Berg and P. A. Quin, Nucl. Phys. **A312** (1978) 1
4) F. Ajzenberg-Selove, Nucl. Phys. **A360** (1981) 1
5) E. K. Warburton and W. T. Pinkston, Phys. Rev. **118** (1960) 733
6) R. J. Peterson and J. J. Hamill, Nucl. Phys. **A362** (1981) 163
7) R. O. Lane *et al.*, Phys. Rev. **C23** (1981) 1883
8) S. F. Mughabghab, M. A. Lone and B. C. Robertson, Phys. Rev. **C26** (1982) 2698
9) M. A. Plum *et al.*, Bull. Am. Phys. Soc. **27** (1982) 530
10) F. Ajzenberg-Selove, Nucl. Phys. **A360** (1981) 1
11) P. Gaillard *et al.*, Nucl. Phys. **A131** (1969) 355
12) R. J. Peterson, J. R. Shepard and R. A. Emigh, Phys. Rev. **C24** (1981) 826
13) R. J. Peterson and J. J. Hamill, Z. Phys. **A305** (1982) 275
14) P. D. Kunz, DWUCK4, a distorted-wave Born approximation code, Univ. of Colorado, unpublished
15) P. D. Kunz, CHUCK2, a coupled-channel reaction code, Univ. of Colorado, unpublished
16) C. M. Vincent and H. T. Fortune, Phys. Rev. **C2** (1970) 782
17) T. H. Curtis, H. F. Lutz, D. W. Heikkinen and W. Bartolini, Nucl. Phys. **A165** (1971) 19

18) S. E. Darden *et al.*, Nucl. Phys. **A208** (1973) 77
19) G. J. Wagner, P. Grabmayr and H. R. Schmidt, Phys. Lett. **113B** (1982)
20) D. F. Geesaman *et al.*, Phys. Rev. **C27** (1983) 1134
21) S. Cohen and D. Kurath, Nucl. Phys. **A101** (1967) 1
22) S. Lie, Nucl. Phys. **A181** (1972) 517
23) H. U. Jäger, H. R. Kissener and R. A. Eramzhian, Nucl. Phys. **A171** (1971) 16
24) D. Dehnhard, Nucl. Phys. **A374** (1982) 377c
25) F. E. Cecil and R. J. Peterson, Phys. Lett. **56B** (1975) 335
26) H. Crannell *et al.*, Nucl. Phys. **A278** (1977) 253
27) H. T. Fortune and G. S. Stephans, Phys. Rev. **C25** (1982) 1
28) M. N. Harakeh and A. E. L. Dieperink, Phys. Rev. **C23** (1981) 2329
29) M. Gai *et al.*, Phys. Rev. Lett. **51** (1983) 646
30) D. A. Resler, P. E. Koehler, H. D. Knox and R. O. Lane, Bull. Am. Phys. Soc. **27** (1982) 628
31) D. J. Millener and D. Kurath, Nucl. Phys. **A255** (1975) 315
32) R. J. Peterson and J. J. Hamill, Phys. Rev. **C22** (1980) 2282
33) G. Morpurgo, Phys. Rev. **131** (1963) 2205
34) R. J. Peterson, Nucl. Phys. **A377** (1982) 41
35) F. J. Kline, H. Crannell, J. T. O'Brien, J. McCarthy and R. R. Whitney, Nucl. Phys. **A209** (1973) 381
36) N. K. Glendenning and M. Veneroni, Phys. Rev. **144** (1966) 839
37) S. Truong and H. T. Fortune, Phys. Rev. **C28** (1983) 977
38) A. M. Bernstein, V. R. Brown and V. A. Madsen, Phys. Lett. **B106** (1981) 259
39) H. Crannell *et al.*, research report of Laboratory of Nuclear Science, Tohuku Univ. (1972), vol. 5
40) D. J. Millener, J. W. Olness, E. K. Warburton and S. S. Hanna, Phys. Rev. **C28** (1983) 497
41) R. J. Peterson, Phys. Scripta, **T5** (1983) 190
42) R. L. Kozub *et al.*, Phys. Rev. **C23** (1981) 1571
43) D. K. Srivastara, Phys. Lett. **130B** (1983) 345